Study of infrared emission spectroscopy for the $B^1\Delta_g$–$A^1\Pi_u$ and $B'^1\Sigma_g^+$–$A^1\Pi_u$ systems of C_2

Wang Chen,[1,a)] Kentarou Kawaguchi,[1,a)] Peter F. Bernath,[2,a)] and Jian Tang[1,b)]
[1]*Graduate School of Natural Science and Technology, Okayama University, 3-1-1 Tsushima-naka, Kita-ku, 700-8530, Okayama, Japan*
[2]*Department of Chemistry and Biochemistry, Old Dominion University, 4541 Hampton Boulevard, Norfolk, Virginia 23529-0126, USA*

(Received 30 November 2015; accepted 15 January 2016; published online 8 February 2016; publisher error corrected 12 February 2016)

Thirteen bands for the $B^1\Delta_g$–$A^1\Pi_u$ system and eleven bands for the $B'^1\Sigma_g^+$–$A^1\Pi_u$ system of C_2 were identified in the Fourier transform infrared emission spectra of hydrocarbon discharges. The $B'^1\Sigma_g^+$ v = 4 and the $B^1\Delta_g$ v = 6, 7, and 8 vibrational levels involved in nine bands were studied for the first time. A direct global analysis with Dunham parameters was carried out satisfactorily for the $B^1\Delta_g$–$A^1\Pi_u$ system except for a small perturbation in the $B^1\Delta_g$ v = 6 level. The calculated rovibrational term energies up to $B^1\Delta_g$ v = 12 showed that the level crossing between the $B^1\Delta_g$ and $d^3\Pi_g$ states is responsible for many of the prominent perturbations in the Swan system observed previously. Nineteen forbidden transitions of the $B^1\Delta_g$–$a^3\Pi_u$ transition were identified and the off-diagonal spin-orbit interaction constant A_{dB} between $d^3\Pi_g$ and $B^1\Delta_g$ was derived as 8.3(1) cm^{-1}. For the $B'^1\Sigma_g^+$–$A^1\Pi_u$ system, only individual band analyses for each vibrational level in the $B'^1\Sigma_g^+$ state could be done satisfactorily and Dunham parameters obtained from these effective parameters showed that the anharmonic vibrational constant $\omega_e x_e$ is anomalously small (nearly zero). Inspection of the RKR (Rydberg-Klein-Rees) potential curves for the $B'^1\Sigma_g^+$ and $X^1\Sigma_g^+$ states revealed that an avoided crossing or nearly avoided crossing may occur around 30 000 cm^{-1}, which is responsible for the anomalous molecular constants in these two states. © *2016 AIP Publishing LLC.* [http://dx.doi.org/10.1063/1.4940907]

I. INTRODUCTION

Recently, progress on the perturbation analysis of C_2 spectra has appeared in several studies for the triplet-quintet ($d^3\Pi_g$–$I^5\Pi_g$) interaction,[1] triplet-triplet ($c^3\Sigma_u^+$–$a^3\Pi_u$) interaction,[2] and singlet-triplet ($X^1\Sigma_g^+$–$b^3\Sigma_g^-$) interaction.[3] These interactions cause prominent perturbations, unusual forbidden triplet-quintet intersystem transitions,[1] forbidden singlet-triplet intersystem transitions,[3] and the observation of a quintet-quintet band.[4] These studies aroused further interest in other C_2 spectra for the many low-lying electronic states (Fig. 1) of this fundamental molecule.

The $B^1\Delta_g$ and $B'^1\Sigma_g^+$ states of C_2 were first predicted by Phillips[5] to explain the perturbations in the v = 4 and 5 vibrational levels of the $d^3\Pi_g$ state. In 1988, the $B^1\Delta_g$–$A^1\Pi_u$ and $B'^1\Sigma_g^+$–$A^1\Pi_u$ band systems were discovered by Douay *et al.*,[6] who observed eight bands of the $B^1\Delta_g$–$A^1\Pi_u$ transition with v up to 5 for the $B^1\Delta_g$ state and six bands of the $B'^1\Sigma_g^+$–$A^1\Pi_u$ transition with v up to 3 for the $B'^1\Sigma_g^+$ state. The molecular constants obtained for $B^1\Delta_g$ were very well behaved, but those for $B'^1\Sigma_g^+$ were anomalous, for example, with a small anharmonic vibrational constant $\omega_e x_e$. It was suspected that interactions with the $X^1\Sigma_g^+$ state were responsible.[6] Recently, *ab initio* potential energy curves were calculated for the low-lying singlet states of C_2 and the anomalous value of $\omega_e x_e$ was reproduced by the theoretical work.[7,8] Other band systems related to the $B^1\Delta_g$ and $B'^1\Sigma_g^+$ states were also observed, such as the $1^1\Delta_u$–$B^1\Delta_g$ transition by REMPI spectroscopy[9] and the $D^1\Sigma_u^+$–$B'^1\Sigma_g^+$ transition by laser induced fluorescence of the photodissociation fragments[10,11] and in solid Ne.[12]

In the study of the Swan system ($d^3\Pi_g$–$a^3\Pi_u$) of C_2, many prominent perturbations in the $d^3\Pi_g$ state could be explained by the interactions at the $d^3\Pi_g$–$b^3\Sigma_g^-$ crossing points, but many unidentified perturbations were suspected due to interactions with the vibrationally excited levels of the $B^1\Delta_g$ and $B'^1\Sigma_g^+$ states.[13] In particular, a puzzling perturbation, which cannot be due to a $b^3\Sigma_g^-$ level, was revealed to cross between the $J = 9$ and $J = 10$ levels of the F_2 spin component for the $d^3\Pi_g$ v = 2 vibrational level with a 1 cm^{-1} perturbation shift to higher wavenumbers and weak extra lines on the lower wavenumber side.[13]

In the work presented here, we identified additional bands with higher vibrational levels for the $B^1\Delta_g$ and $B'^1\Sigma_g^+$ states. As a result, the $B^1\Delta_g$ v = 9 level is found to be responsible for perturbing the $d^3\Pi_g$ v = 2 level, and the extra lines observed previously[13] were just the forbidden transitions with considerable intensity borrowed from the allowed transitions. For the $B'^1\Sigma_g^+$ state, the anomalous anharmonic vibrational constant $\omega_e x_e$ is likely caused by an avoided crossing between the $B'^1\Sigma_g^+$ and $X^1\Sigma_g^+$ potential curves.

a)Electronic addresses: sc19321@s.okayama-u.ac.jp, okakent@okayama-u.ac.jp, and pbernath@odu.edu
b)Author to whom correspondence should be addressed. Electronic mail: jtang@okayama-u.ac.jp. Tel: +81(86)251-7849. Fax: +81(86)251-7853.

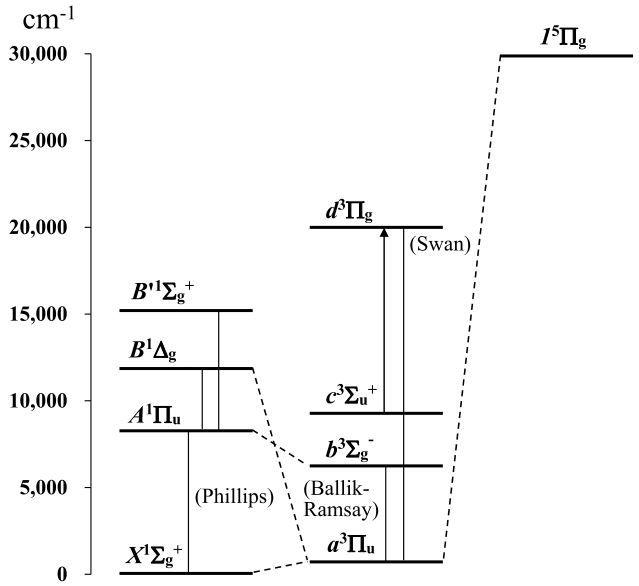

FIG. 1. Low-lying electronic states of C_2 below 30 000 cm^{-1} and observed transition systems (vertical solid lines) within the same multiplicity. Intersystem forbidden transitions (dashed lines) were observed recently for $1^5\Pi_g$–$a^3\Pi_u$ (Ref. 1), $X^1\Sigma_g^+$–$a^3\Pi_u$ and $A^1\Pi_u$–$b^3\Sigma_g^-$ (Ref. 3), and $B^1\Delta_g$–$a^3\Pi_u$ in the present work.

II. SPECTRAL ASSIGNMENT

During our previous study,[3] we noticed some new bands around 3500 cm^{-1} in the Fourier transform infrared (FTIR) emission spectrum of C_2 observed by a positive column discharge in the CH_4 and He mixture with a spectral resolution of 0.02 cm^{-1}.[14] Using the molecular constants of Douay *et al.*,[6] we could assign these bands easily to v = 0-2, 1-3, 2-4, and 3-5 of the $B'^1\Sigma_g^+$–$A^1\Pi_u$ system. The variation of the line intensity for these $\Delta v = -2$ bands indicated that the v = 4-6 band might be observable, but the 5-7 band might be too weak to be seen. Using the equilibrium molecular constants of Douay *et al.* derived for $B'^1\Sigma_g^+$,[6] we estimated the band position for the v = 4-6 band and were able to assign the transition around 3470 cm^{-1}, about 5.8 cm^{-1} lower than the predicted. A portion of the spectrum mainly showing the Q-branch of the v = 4-6 band is shown in Fig. 2.

TABLE I. Assigned $B'^1\Sigma_g^+$–$A^1\Pi_u$ and $B^1\Delta_g$–$A^1\Pi_u$ bands for C_2.

	Δv	v′-v″(J_{max})				
$B'^1\Sigma_g^+$–$A^1\Pi_u$	−2	0-2(30)	1-3(32)	2-4(30)	3-5(28)	4-6(26)
	−1	0-1(37)[a]	1-2(41)[a]	2-3(40)	3-4(34)	4-5(26)
	0	0-0(41)[a]	1-1(35)	2-2(26)		
	1	1-0(40)[a]	2-1(38)[a]	3-2(34)[a]	4-3(28)	
$B^1\Delta_g$–$A^1\Pi_u$	−1	0-1(26)[a]				
	0	0-0(40)[a]	1-1(27)	4-4(15)	5-5(24)	
	1	1-0(46)[a]	2-1(37)[a]	3-2(34)[a]		
	2	2-0(40)	3-1(39)[a]	4-2(36)[a]	5-3(31)	6-4(26)
	3	3-0(34)	4-1(33)	5-2(33)[a]	6-3(36)	7-4(34) 8-5(24)
	4	6-2(24)	7-3(33)			

[a]Bands assigned previously by Douay *et al.*[6] were extended to higher J values.

With the newly determined molecular constants for the $B'^1\Sigma_g^+$ v = 4 level, as shown later in Table VII, we extended the $B'^1\Sigma_g^+$–$A^1\Pi_u$ assignment to the higher wavenumber region by using two previously observed spectra by Douay *et al.*[15] and could assign the v = 2-3, 3-4, and 4-5 bands around 5000 cm^{-1}, the v = 1-1, and 2-2 bands around 7000 cm^{-1}, and the v = 4-3 band around 8000 cm^{-1}, as summarized in Table I. Among these assigned bands, the wavenumbers for three bands with v = 4 for the $B'^1\Sigma_g^+$ state are listed in Table II.

For the $B^1\Delta_g$–$A^1\Pi_u$ system, seven bands up to v = 5 for the $B^1\Delta_g$ state were assigned in this work using the molecular constants of Douay *et al.*[6] In addition, six bands with v = 6, 7, and 8 for the $B^1\Delta_g$ state were assigned using the equilibrium molecular constants of Douay *et al.*[6] and the transition wavenumbers are listed in Table III. All the assigned $B^1\Delta_g$–$A^1\Pi_u$ bands are summarized in Table I with vibrational quantum numbers.

III. ANALYSIS

For the $B^1\Delta_g$–$A^1\Pi_u$ system, we first analyzed the individual vibrational levels up to v = 8 of the upper $B^1\Delta_g$ state by fixing Dunham parameters of the lower $A^1\Pi_u$ state to those of our previous work,[3] as shown in Table IV. These effective molecular constants are compared with those of Douay *et al.* Then, a direct global analysis using Dunham parameters for

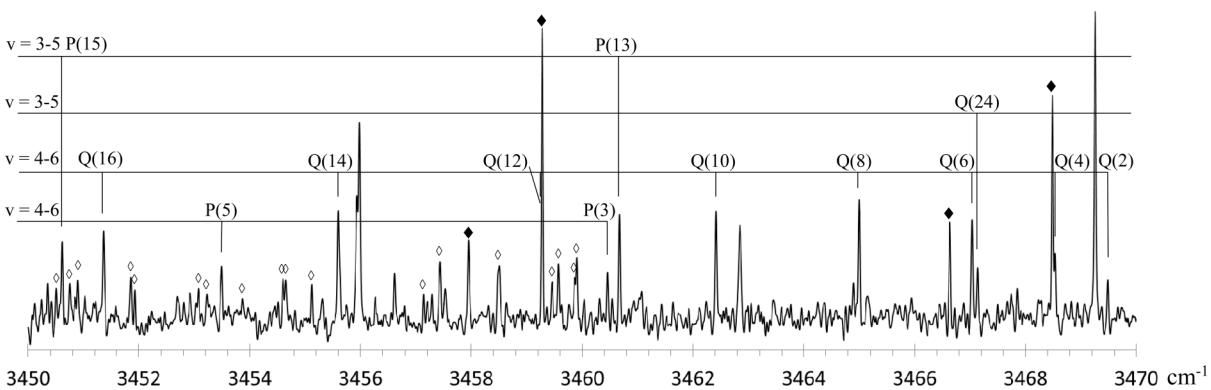

FIG. 2. A portion of the spectrum showing the Q- and P-branches of v = 4-6 and v = 3-5 bands for the $B'^1\Sigma_g^+$–$A^1\Pi_u$ system. The lines marked with ♦ belong to the v = 0-0 band for the $B^1\Delta_g$–$A^1\Pi_u$ system. The lines marked with ◊ belong to the $b^3\Sigma_g^-$–$a^3\Pi_u$ system as assigned in Ref. 3.

TABLE II. $B'^1\Sigma_g^+$–$A^1\Pi_u$ transitions with $B'^1\Sigma_g^+$ v = 4 (in cm^{-1}). Observed minus calculated in units of 10^{-4} cm^{-1}.

4-3 band							
J	R_{ee}	O-C	P_{ee}	O-C	*J*	Q_{ef}	O-C
1	7935.7065	−7	7927.0852	−23			
3	7940.2439	−82[a]	7920.1429	12	2	7929.4766	−31
5	7943.8346	8	7912.2365	−10	4	7927.8044	76[a]
7	7946.4517	13			6	7925.1512	−6
9	7948.0995	−4	7893.5547	−26	8	7921.5433	−6
11	7948.7802	3	7882.7847	24	10	7916.9723	−1
13	7948.4856	26	7871.0503	−8	12	7911.4329	−35
15	7947.2195	−31	7858.3675	34	14	7904.9334	−13
17	7944.9710	−102[a]	7844.7187	−28	16	7897.4643	−22
19	7941.7607	−13	7830.1269	30	18	7889.0281	−29
21	7937.5740	102[a]	7814.5686	−33	20	7879.6250	−28
23			7798.0677	9	22		
25					24	7857.9194	9
27					26	7845.6143	0[b]
29					28	7832.3132	−332[a]

4-5 band							
J	R_{ee}	O-C	P_{ee}	O-C	*J*	Q_{ef}	O-C
3			4922.5533	56[b]	2	4931.6808	35
5	4946.8684	34	4915.2708	22	4	4930.4824	17
7	4950.3749	−97[a]	4907.3122	22	6	4928.6011	12
9	4953.2198	48[b]	4898.6774	49[b]	8	4926.0360	19
11	4955.3594	53[b]	4889.3702	137[a]	10	4922.7859	32
13	4956.8010	15	4879.3641	17	12	4918.8476	28
15	4957.5493	0	4868.6933	25	14	4914.2211	16
17	4957.6022	7	4857.3369	−50[b]	16	4908.9100	39
19	4956.9541	−4	4845.3193	29	18	4902.9024	−13
21	4955.6159	87[a]	4832.6156	3	20	4896.2108	−15
23	4953.5596	6	4819.2405	5	22	4888.8309	−9
25	4950.8076	−25	4805.1938	14	24	4880.7637	6
27			4790.4844	91[a]	26	4872.0100	24

4-6 band							
J	R_{ee}	O-C	P_{ee}	O-C	*J*	Q_{ef}	O-C
1	3475.5108	−12					
3	3480.5759	−34	3460.4609	−80[a]	2	3469.4865	−70[a]
5	3485.0968	−47[b]	3453.4982	−69[b]	4	3468.5426	5
7	3489.0763	−2	3445.9978	−41	6	3467.0421	−45[b]
9	3492.4971	−55[b]	3437.9589	−11	8	3465.0058	−6
11	3495.3701	−73[b]	3429.3734	−64[b]	10	3462.4156	−52[b]
13	3497.6919	−70[b]	3420.2557	−61[b]	12	3459.2837	−52[b]
15	3499.4558	−93[a]	3410.5993	−72[b]	14	3455.5970	−129[a]
17	3500.6631	−109[a]	3400.4042	−102[a]	16	3451.3876	45[b]
19			3389.6620	−242[a]	18	3446.6157	78[a]
21					20	3441.2916	76[b]
23					22	3435.4147	30
25					24	3428.9931	12
27					26	3422.0235	−26

[a]Not included in the least-squares fit.
[b]With reduced weight in the least-squares fit.

TABLE III. $B^1\Delta_g$–$A^1\Pi_u$ transitions with v = 6, 7, 8 for $B^1\Delta_g$ (in cm^{-1}). Observed minus calculated in units of 10^{-4} cm^{-1}.

6-2 band						
J	R_{ff}	O-C	Q_{ef}	O-C	P_{ff}	O-C
2	8419.0748	−89[a]				
4	8421.4083	−45	8407.8806	25		
6	8421.9700	−68	8403.0299	−26		
8	8420.7817	70[a]	8396.4203	−48	8374.7674	−102[b]
10	8417.8035	−17	8388.0514	−47	8360.9955	−104[b]
12	8413.0642	−33	8377.9212	−43	8345.4780	−10
14	8406.5632	28	8366.0323	−14	8328.1907	−75[a]
16	8398.2903	72[a]				
18	8388.2335	−11	8336.9654	−20		
20	8376.4130	−10	8319.7947	10		
22			8300.8606	6		
24	8347.4548	15	8280.1677	7		

J	R_{ee}	O-C	Q_{fe}	O-C	P_{ee}	O-C
1	8417.2533	−47				
3	8420.4716	5	8409.6491	67		
5	8421.9140	−73[a]	8405.6904	91[b]		
7	8421.6097	23	8399.9599	1		
9	8419.5304	22	8392.4759	−22	8368.1259	−26
11	8415.6777	−51	8383.2315	−47	8353.4809	−62
13	8410.0688	−12	8372.2278	−68	8337.0880	−45
15	8402.6879	−11			8318.9449	−16
17	8393.5351	−36	8344.9445	−81[a]	8299.0568	65
19	8382.6403	221[b,c]	8328.6993	264[b,c]		
21	8369.9332	65[b,c]				
23	8355.4651	18	8290.8434	54		
25	8339.2296	24				

6-3 band						
J	R_{ff}	O-C	Q_{ef}	O-C	P_{ff}	O-C
2			6875.5049	−18		
4			6872.6615	−28		
6	6887.1473	53	6868.1989	12	6851.9451	−126[b]
8	6886.4590	24	6862.1102	31	6840.4594	−2
10	6884.1376	−43	6854.3921	−6	6827.3463	37
12	6880.1815	−152[b]	6845.0543	−4	6812.6119	37
14	6874.6135	−67	6834.0977	42	6796.2606	26
16	6867.4147	32	6821.5088	−5	6778.2945	10
18	6858.5884	188[b]	6807.3029	4	6758.7167	3
20	6848.0939	0	6791.4734	−2	6737.5210	−73[a]
22	6835.9854	19	6774.0225	−6	6714.7292	−18
24	6822.2373	−5	6754.9347	−168[b]	6690.3566	304[b]
26			6734.2685	91[b]	6664.3182	23
28	6789.8402	25	6711.9436	−38	6636.7046	29
30			6688.0155	−8	6607.4828	−30
34			6635.2968	−28		
36			6606.5182	26		

J	R_{ee}	O-C	Q_{fe}	O-C	P_{ee}	O-C
1	6881.7340	−2				
3	6885.1194	−1	6874.2882	−26		
5	6886.8806	9	6870.6442	45		
7	6887.0170	34	6865.3810	150[b]		
9	6885.5328	127[b]	6858.4781	81[a]		
11	6882.4059	76[a]	6849.9518	1		
13			6839.8105	−10		
15	6871.2693	39	6828.0553	56	6787.5332	103[b]

TABLE III. (*Continued.*)

6-3 band						
J	R_{ee}	O-C	Q_{fe}	O-C	P_{ee}	O-C
17	6863.2533	7	6814.6385	−280[b]	6768.7573	−70[a]
19	6853.6072	−6	6799.6637	12	6748.3950	−3
21	6842.3405	104[b]			6726.4093	−84[a]
23			6764.7885	−51	6702.8448	116[b]
25	6814.8653	−80[a]	6744.9513	215[b]	6677.6380	−55
27			6723.4323	−148[b]	6650.8515	11
29			6700.3409	−54	6622.4574	14
31			6675.6290	10		

6-4 band						
J	R_{ff}	O-C	Q_{ef}	O-C	P_{ff}	O-C
2	5372.5102	−64	5364.3910	−35		
4	5375.3340	47	5361.7978	32		
6	5376.6647	114[b]	5357.7117	27		
8	5376.4908	32	5352.1454	74		
10	5374.8346	36	5345.0915	96[b]		
12	5371.6865	37	5336.5430	22		
14	5367.0457	38	5326.5176	25		
18			5302.0113	−4		
20			5287.5392	43		
24			5254.1273	−69		
			5235.2164	49		

J	R_{ee}	O-C	Q_{fe}	O-C	P_{ee}	O-C
3	5374.1167	54	5363.2867	42		
5			5359.9451	20		
7	5376.7696	23	5355.1249	51		
9	5375.8719	92[b]				
11			5341.0138	−80[b]		
13	5369.5796	−36				
15			5320.9910	2	5280.4659	19
17			5308.7474	−39		
21			5279.8274	6		
23			5263.1381	−48		
25			5244.9620	−168[b]		

7-3 band						
J	R_{ff}	O-C	Q_{ef}	O-C	P_{ff}	O-C
2	8131.7220	−109[b]	8123.7209	77[a]		
4	8133.9857	−101[b]	8120.6340	22		
6	8134.4811	−138[b]	8115.7894	−2		
8	8133.2259	−32	8109.1847	−21		
10	8130.1935	−38	8100.8219	−18	8074.1224	74[a]
12	8125.3976	−11	8090.7020	15		
14			8078.8176	1		
16	8110.4927	−42	8065.1733	−17	8022.5010	−44
18	8100.3836	−86[b]			8001.8092	74[a]
20	8088.5186	15	8032.6116	−19	7979.3554	46
22	8074.8708	−3	8013.6907	−48	7955.1540	−2
24	8059.4592	58	7993.0199	−2	7929.2076	−62
26			7970.5750	−129[b]		
28			7946.3943	−52		
30			7920.4535	−24		
32			7892.7557	−20		

J	R_{ee}	O-C	Q_{fe}	O-C	P_{ee}	O-C
1	8129.9440	33				
3	8133.0832	−38				

TABLE III. (*Continued.*)

7-3 band						
J	R_{ee}	O-C	Q_{fe}	O-C	P_{ee}	O-C
5	8134.4811	95[b]	8118.4356	−9		
7	8134.0921	−12	8112.7153	−36	8094.0049	−87[b]
9	8131.9513	2	8105.2453	29	8081.2181	179[b]
11	8128.0408	−32	8096.0049	−23	8066.6339	3
13	8122.3719	9	8085.0134	−1	8050.3192	39
15	8114.9309	−3	8072.2587	−29	8032.2472	3
17	8105.7164	−73[a]	8057.7531	11		
19	8094.7502	25	8041.4792	−59		
21			8023.4640	27	7967.5617	40
23	8067.4971	97[b]	8003.6790	−22	7942.4932	−124[b]
25	8051.2069	51	7982.1481	28		
27			7958.8547	2		
29			7933.8126	34		
33			7878.4563	−22		

7-4 band						
J	R_{ff}	O-C	Q_{ef}	O-C	P_{ff}	O-C
2			6612.5997	−14		
4	6623.1250	−11	6609.7700	79[a]	6599.0778	79[a]
6	6624.0028	−34	6605.3040	31	6589.2615	−43
8	6623.2573	−27	6599.2035	−143[b]	6577.8340	−94[b]
10	6620.8915	50	6591.5126	−3	6564.7979	−63
12	6616.8841	−6	6582.1829	−36	6550.1511	14
14	6611.2658	120[b]	6571.2378	−13	6533.8874	58
16			6558.6574	−136[b]	6515.9983	−31
18	6595.1021	7	6544.4823	−5		
20	6584.5771	−14	6528.6759	10		
22	6572.4254	18	6511.2491	11	6452.7033	−34
24			6492.1992	−36		
26	6543.2208	52	6471.5395	−5		
30	6507.4760	23				
32			6399.8557	11		
34			6372.7304	2		

J	R_{ee}	O-C	Q_{fe}	O-C	P_{ee}	O-C
3	6622.0801	13	6611.3914	48		
5	6623.7789	38	6607.7417	18		
7	6623.8584	114[b]	6602.4731	4	6583.7698	24
9	6622.2947	10	6595.5789	−61	6571.5501	73[a]
11	6619.1286	145[b]	6587.0777	5	6557.7075	39
13			6576.9502	5	6542.2606	91[b]
15	6607.8440	−283[b]	6565.2016	−11	6525.1873	−7
17	6599.8046	−39	6551.8497	129[b]	6506.5161	13
19	6590.1201	51	6536.8515	−9		
21	6578.7928	15	6520.2498	−3	6464.3433	−31
23	6565.8472	104[b]	6502.0466	161[b]	6440.8670	121[b]
25	6551.2540	32	6482.1973	30		
27	6535.0318	−10			6389.0720	52
29	6517.1835	10	6437.6691	−63		
33	6476.5711	−124[b]				

8-5 band						
J	R_{ff}	O-C	Q_{ef}	O-C	P_{ff}	O-C
2	6359.5396	−40				
4	6362.0050	193[b]	6348.7944	21		
6			6344.3339	−50		
8	6362.0050	35	6338.2719	55		
10	6359.5829	97[b]	6330.5763	13		

TABLE III. (*Continued.*)

8-5 band						
J	R_{ff}	O-C	Q_{ef}	O-C	P_{ff}	O-C
12			6321.2661	11	6289.6301	−76[a]
14	6349.8431	35	6310.3464	95[b]	6273.4552	−20
16	6342.5326	−1			6255.6658	−18
18	6333.5957	−24				
20			6267.8552	68		
22			6250.4544	16		
24			6231.4410	−11		
J	R_{ee}	O-C	Q_{fe}	O-C	P_{ee}	O-C
3	6360.9681	−15	6350.4150	10		
5	6362.6131	91[b]	6346.7785	49		
7	6362.6131	−38	6341.5182	27		
9	6360.9681	−392[b]	6334.6380	−19		
11			6326.1461	−9	6297.1401	−86[a]
13	6352.9197	28	6316.0454	82[a]	6281.7767	−59
15	6346.4328	−15			6264.8165	84[a]
17	6338.3321	63				
19			6276.0121	13		

[a]With reduced weight in the least-squares fit.
[b]Not included in the least-squares fit.
[c]With known perturbation in the $A^1\Pi_u$ state.

the energy term of the $B^1\Delta_g$ state as

$$E = T_e + \omega_e\left(v+\frac{1}{2}\right) - \omega_e x_e\left(v+\frac{1}{2}\right)^2 + \omega_e y_e\left(v+\frac{1}{2}\right)^3 + \omega_e z_e\left(v+\frac{1}{2}\right)^4 + \left(B_e - \alpha_e\left(v+\frac{1}{2}\right) + \gamma_e\left(v+\frac{1}{2}\right)^2 + \delta_e\left(v+\frac{1}{2}\right)^3\right) J(J+1) - \left(D_e + \beta_e\left(v+\frac{1}{2}\right) + \zeta_e\left(v+\frac{1}{2}\right)^2\right) J^2(J+1)^2 + H_e J^3(J+1)^3 \quad (1)$$

was carried out satisfactorily for up to v = 8, as shown in Table V and in the supplementary material[16] for the detailed fit. For comparison, the results of Douay *et al.*,[6] which were derived from the effective molecular constants for the individual levels up to v = 5, are also shown in Table V. Three higher order constants $\omega_e z_e$, δ_e, and H_e were obtained in this work. Some transitions with J lower than 25 for $B^1\Delta_g$ v = 6 showed a small perturbation of about 0.02 cm^{-1} and were not included in the global fit. We consider that this perturbation is caused by the spin-orbit interaction with the nearby v = 0 level of the $d^3\Pi_g$ state (about 170 cm^{-1} higher). In Sec. IV, we will show that many perturbations observed previously can be identified as interactions near level crossings between the $B^1\Delta_g$ and $d^3\Pi_g$ states.

In contrast to the $B^1\Delta_g$ state, the molecular constants for the $B'^1\Sigma_g^+$ state are anomalous as pointed out by Douay *et al.*[6] Effective molecular constants for the individual vibrational levels up to v = 4 of the $B'^1\Sigma_g^+$ state were obtained as shown in Table VI. In comparison with the results of Douay *et al.*[6] for v up to 3, all the constants are in good agreement except for the H_v constants, since we have extended the analysis to higher J values. We also tried a global fit for the 17 bands of the $B'^1\Sigma_g^+$–$A^1\Pi_u$ system using Dunham parameters, but the standard deviation of about 0.3 cm^{-1} for the fit was not acceptable. Therefore, a fit for the effective molecular constants listed in Table VI led to the Dunham parameters (with the same definition as the above for the $B^1\Delta_g$ state) as shown in Table VII. The present result with v up to 4 showed that $\omega_e y_e$, γ_e, and even $\omega_e x_e$ (with a value of 0.10(11) cm^{-1} if fitted) were indeterminable, and we fixed them to zero. In the fit of Douay *et al.* with v up to 3, they obtained exact values for the four Dunham parameters from four vibrational levels up to v = 3.[6] If $\omega_e y_e$ is fixed to zero, $\omega_e x_e$ becomes very small and indeterminable. So we listed also a fit for v up to 3 with $\omega_e x_e$ and $\omega_e y_e$ fixed to zero in Table VII, which gives a much better prediction (about 0.2 cm^{-1} shift) for the band positions involved with v = 4 of the $B'^1\Sigma_g^+$ state. The ζ_e constant for the $(v+1/2)^2$ term of the centrifugal distortion expansions was required to account for the nonlinear dependence of D_v on $v+1/2$ in Table VI. The anomalously large value of ζ_e,

TABLE IV. Effective molecular constants for the $B^1\Delta_g$ state (in cm^{-1}).[a]

	T_v[b]		B_v		$D_v \times 10^6$	
v	This work	Douay *et al.*[c]	This work	Douay *et al.*[c]	This work	Douay *et al.*[c]
0	11 859.0998(3)	11 859.0980(2)	1.455 264 5(13)	1.455 273 3(21)	6.3186(10)	6.3259(13)
1	13 243.6383(3)	13 243.6377(3)	1.438 423 1(10)	1.438 427 7(24)	6.3376(5)	6.3420(16)
2	14 605.3101(4)	14 605.3115(4)	1.421 551 4(16)	1.421 552 1(28)	6.3613(12)	6.3575(24)
3	15 944.1788(4)	15 944.1799(4)	1.404 644 0(19)	1.404 642 0(30)	6.3801(17)	6.3671(29)
4	17 260.3029 (4)	17 260.3030(12)	1.387 705 0(22)	1.387 721 0(80)	6.3900(21)	6.4035(85)
5	18 553.7491(6)	18 553.7486(9)	1.370 744 3(38)	1.370 739 3(81)	6.4115(41)	6.388(14)
6	19 824.5495(6)		1.353 798 5(31)		6.4578(30)	
7	21 072.8585(6)		1.336 724 9(33)		6.4474(32)	
8	22 298.673(3)		1.319 668(28)		6.452(43)	

[a]Numbers in parentheses are one standard deviation in the last digits.
[b]Energy term values relative to $X^1\Sigma_g^+$ v = 0.
[c]Reference 6.

TABLE V. Dunham parameters for the $B^1\Delta_g$ state (in cm^{-1}).[a]

	This work[b]	Douay *et al.*[c]
T_e	12 082.343 55(54)	12 082.3360(40)
ω_e	1 407.450 92(77)	1 407.465 29(134)
$\omega_e x_e$	11.471 37(34)	11.479 37(60)
$\omega_e y_e$	0.008 524(58)	0.010 256(73)
$\omega_e z_e$	0.000 128 8(34)	
B_e	1.463 673 2(16)	1.463 685 3(34)
α_e	0.016 809 25(92)	0.016 816 1(35)
$\gamma_e \times 10^5$	−1.712(25)	−1.503(72)
$\delta_e \times 10^7$	1.81(21)	
$D_e \times 10^6$	6.306 3(16)	6.318 8(19)
$\beta_e \times 10^8$	1.778(25)	1.492(113)
$H_e \times 10^{12}$	−1.75(44)	

[a]Numbers in parentheses are one standard deviation in the last digits.
[b]Obtained directly by a global fit for 1261 transitions with a standard deviation of 0.0024 cm^{-1}.
[c]Obtained from the effective constants (Ref. 6).

TABLE VII. Dunham parameters for the $B'^1\Sigma_g^+$ state (in cm^{-1}).[a]

	This work		Douay *et al.*[b]	
T_e	15 410.33(36)	15 410.77(59)	15 409.1390[c]	15 410.36(55)[d]
ω_e	1 420.36 (13)	1 419.84(55)	1 424.118 90[c]	1 420.35(24)[d]
$\omega_e x_e$	0 (fixed)	0.10(11)	2.571 13[c]	0 (fixed)
$\omega_e y_e$	0 (fixed)	0 (fixed)	0.463 98[c]	0 (fixed)
B_e	1.479 67(82)		1.481 01(30)	
α_e	0.009 43(29)		0.011 75(46)	
$\gamma_e \times 10^5$	0 (fixed)		67(14)	
$D_e \times 10^6$	6.785(103)		6.859 6(136)	
$\beta_e \times 10^6$	−0.336(97)		−0.158 1(143)	
$\zeta_e \times 10^6$	0.100 2(189)			

[a]Numbers in parentheses are one standard deviation in the last digits.
[b]Reference 6.
[c]Exact values solved from the four T_v constants of v = 0–3 in Ref. 6.
[d]Obtained by fitting from the four T_v constants of v = 0–3 for comparison in this work.

TABLE VIII. Calculated values for $\omega_e x_e$ of C_2 from the Pekeris relation (cm^{-1}).

	Calculated	Experimental	Expt.-calculated
$X^1\Sigma_g^+$	13.0	14.6(1)[a]	1.6
$A^1\Pi_u$	12.1	12.079(2)[b]	0.0
$a^3\Pi_u$	11.9	11.6490(4)[b]	−0.3
$b^3\Sigma_g^-$	11.6	11.1355(4)[b]	−0.5
$B^1\Delta_g$	11.8	11.4742(4)[c]	−0.3
$B'^1\Sigma_g^+$	6.0	0.1(1)[c]	−5.9

[a]From Table IX.
[b]Taken from Ref. 3.
[c]From the present study.

which has the same magnitude as the β_e constant (Table VII), and also the small value of α_e, when compared with the values of about 0.016 cm^{-1} for other electronic states of C_2, may mean that there is a vibrational perturbation of the $B'^1\Sigma_g^+$ state.

IV. DISCUSSION

A. Interaction between the $B'^1\Sigma_g^+$ and $X^1\Sigma_g^+$ potential curves

The anharmonic constants $\omega_e x_e$ can be estimated using the Pekeris relation[17] as $\omega_e x_e = B_e(\omega_e\alpha_e/(6B_e^2) + 1)^2$, which holds very nicely for all the low-lying electronic states of C_2, as shown in Table VIII, except for the $B'^1\Sigma_g^+$ and $X^1\Sigma_g^+$ states, as pointed out by Douay *et al.*[6] Therefore, the anomalously small $\omega_e x_e \approx 0.1(1)$ cm^{-1} obtained for $B'^1\Sigma_g^+$ must be an effective value, which implies that some interaction with other electronic states distorted the anharmonic potential curve back to a near-harmonic shape, at least up to v = 4. A possible mechanism for this distortion is considered below.

The vibrational term values for the $X^1\Sigma_g^+$ state are known up to v = 9.[18] In our previous global analysis,[3] we fitted the bands up to v = 6 with $G(v) = \omega_e\left(v + \frac{1}{2}\right) - \omega_e x_e\left(v + \frac{1}{2}\right)^2 + \omega_e y_e\left(v + \frac{1}{2}\right)^3 + \omega_e z_e\left(v + \frac{1}{2}\right)^4 + \omega_e a_e\left(v + \frac{1}{2}\right)^5$. Although the Dunham parameters obtained reproduced the transition wavenumbers accurately up to v = 6, the calculated term value of v = 9 is about 1.2 cm^{-1} away from the observed value. To simulate the potential curve to higher vibrational energy, we refit the term values up to v = 9 with a G(v) expansions with just four terms, as shown in Table IX, which reproduces the vibrational term values to within 0.2 cm^{-1}. The next expansion constant $\omega_e a_e$ was not determinable, so was not included in the fit.

The Dunham parameters of the $B'^1\Sigma_g^+$ and $X^1\Sigma_g^+$ states in Tables VII and IX were input to Le Roy's "RKR" program[19]

TABLE VI. Effective molecular constants for the individual vibrational levels of the $B'^1\Sigma_g^+$ state (in cm^{-1}).[a]

	T_v[b]		B_v		$D_v \times 10^6$		$H_v \times 10^{10}$	
v	This work	Douay *et al.*[c]	This work	Douay *et al.*[c]	This work	Douay *et al.*[c]	This work	Douay *et al.*[c]
0	15 196.5142(4)	15 196.5116(4)	1.475 267 1(32)	1.475 312 4(42)	6.6531(54)	6.7810(95)	1.260(24)	2.220(66)
1	16 616.9992(4)	16 616.9962(4)	1.464 779 1(29)	1.464 823 0(52)	6.5022(50)	6.621(14)	1.234(24)	2.17(11)
2	18 036.5190(4)	18 036.5144(8)	1.456 062 1(28)	1.456 135(11)	6.5162(49)	6.744(35)	1.382(22)	3.38(30)
3	19 457.5828(4)	19 457.5801(9)[d]	1.447 840 5(42)	1.447 863(17)	6.9132(99)	6.881(63)	2.222(62)	
4	20 878.0255(6)		1.436 645 9(96)		7.272(37)		3.51(35)	

[a]Numbers in parentheses are one standard deviation in the last digits.
[b]Energy term values relative to $X^1\Sigma_g^+$ v = 0.
[c]Reference 6.
[d]Corrected to 19 457.8501(9) cm^{-1} which was misprinted in Ref. 6.

TABLE IX. Derived Dunham parameters and vibrational term values for the $X^1\Sigma_g^+$ state (cm^{-1}).

ω_e	$\omega_e x_e$	$\omega_e y_e$	$\omega_e z_e$
1856.62(36)	14.61(14)	0.141(22)	−0.0260(11)
v	T_v		Observed-calculated[a]
0	0		0.07
1	1 827.4849(2)[b]		−0.17
2	3 626.6835(2)[b]		0.02
3	5 396.6892(4)[b]		0.14
4	7 136.3507(6)[b]		0.06
5	8 844.1241(11)[b]		−0.10
6	10 517.9659(39)[b]		−0.11
7	12 154.9615(29)[c]		0.03
8	13 751.3944(38)[c]		0.12
9	15 302.8952(46)[c]		−0.06

[a]Observed T_v minus calculation from the above constants.
[b]Determined from the observation in Ref. 15.
[c]Determined from the observation in Ref. 18.

to calculate the RKR (Rydberg-Klein-Rees) potential curves, which are shown as the solid lines in Fig. 3. When we assume that the anharmonic expansion constants $\omega_e x_e$ in both the $B'^1\Sigma_g^+$ and $X^1\Sigma_g^+$ states are 12 cm^{-1} as for most of the other electronic states, the dashed curves in Fig. 3 were obtained, which cross near the energy of 30 000 cm^{-1}. Since the $B'^1\Sigma_g^+$ and $X^1\Sigma_g^+$ states have the same symmetry, the solid RKR potential curves can be regarded as the result of an avoided crossing[20] of the dashed curves in Fig. 3, and the anomalous $\omega_e x_e$ values for the $B'^1\Sigma_g^+$ and $X^1\Sigma_g^+$ states, especially the

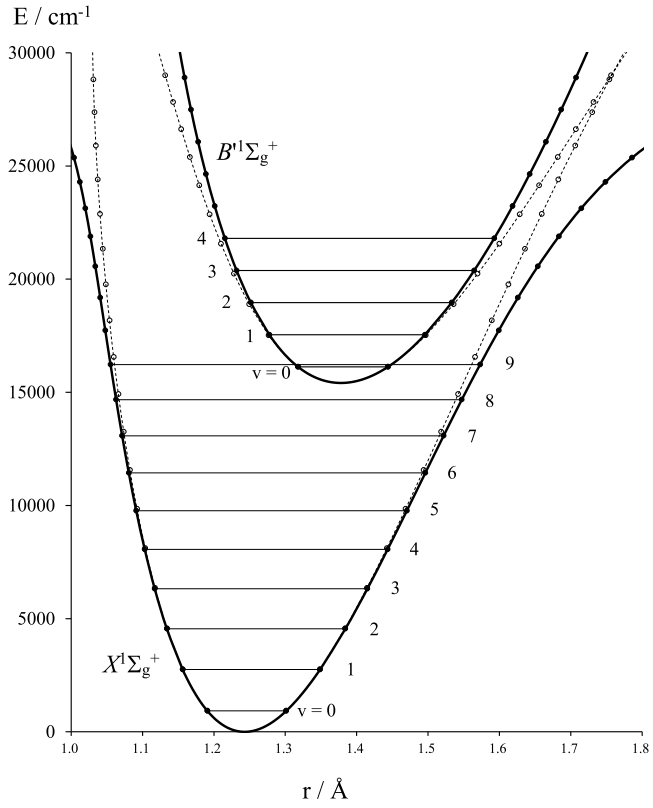

FIG. 3. The RKR potentials for the $X^1\Sigma_g^+$ and $B'^1\Sigma_g^+$ states. The solid lines are calculated with the Dunham parameters in Tables IX and VII. They may cross around 30 000 cm^{-1} in the case of $\omega_e x_e = 12$ cm^{-1} (a regular value in C_2) and are shown as dashed lines.

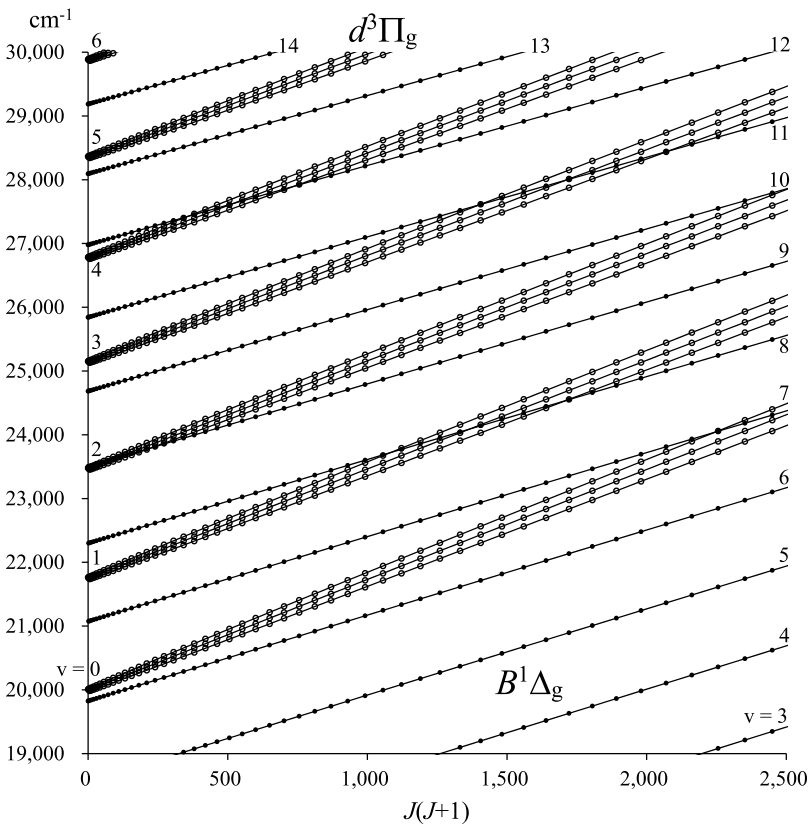

FIG. 4. Rovibrational term values for the $d^3\Pi_g$ state (line with open circles) and the $B^1\Delta_g$ state (line with solid dots).

TABLE X. Calculated and observed perturbations around level crossings (in cm^{-1}).

$B^1\Delta_g$			$d^3\Pi_g$								
v	J	E_B[a]	v	J	F	E_d[b]	Δ[c]	$\lvert\langle v_B \rvert v_d\rangle\rvert$[d]	W[e]	δ[f]	r(%)[g]
7	50	24 439.58	0	50	2	24 397.74	41.84	0.128	1.68	0.03	0.1
7	51	24 572.51	0	51	2	24 574.74	−2.24	0.128	1.68	0.42 (0.56)	16.2
7	52	24 707.90	0	52	2	24 749.79	−41.89	0.128	1.68	0.03	0.1
7	54	24 986.06	0	54	1	24 932.46	53.60	0.128	1.68	0.02	0.1
7	55	25 128.80	0	55	1	25 114.51	14.29	0.128	1.68	0.08	0.6
7	56	25 273.99	0	56	1	25 304.28	−30.29	0.128	1.68	0.04	0.2
8	35	23 951.20	1	35	2	23 909.61	41.59	0.221	2.83	0.08	0.2
8	36	24 045.01	1	36	2	24 030.91	14.10	0.221	2.83	0.23 (0.27)	1.9
8	37	24 141.36	1	37	2	24 158.86	−17.50	0.221	2.83	0.19 (0.37)	1.3
8	38	24 240.23	1	38	2	24 286.71	−46.48	0.221	2.83	0.07	0.2
8	40	24 445.55	1	40	1	24 420.10	25.45	0.221	2.83	0.13	0.6
8	41	24 551.98	1	41	1	24 555.16	−3.17	0.221	2.83	0.84 (0.74)[h]	20.7
8	42	24 660.92	1	42	1	24 696.04	−35.12	0.221	2.83	0.10	0.3
9	6	23 556.79	2	6	2	23 534.49	22.29	0.272	3.48	0.23 (0.11)	1.2
9	7	23 575.01	2	7	2	23 558.61	16.40	0.272	3.48	0.30 (0.18)	2.1
9	8	23 595.84	2	8	2	23 585.24	10.60	0.272	3.48	0.46 (0.34)	4.7
9	9	23 619.27	2	9	2	23 616.31	2.96	0.272	3.48	1.21 (1.13)	27.9
9	10	23 645.30	2	10	2	23 649.73	−4.43	0.272	3.48	0.95 (0.91)	17.9
9	11	23 673.92	2	11	2	23 687.70	−13.78	0.272	3.48	0.36 (0.40)	2.9
9	12	23 705.14	2	12	2	23 727.88	−22.75	0.272	3.48	0.22 (0.23)	1.1
9	12	23 705.14	2	12	1	23 683.57	21.57	0.272	3.48	0.23 (0.18)	1.3
9	13	23 738.95	2	13	1	23 724.64	14.31	0.272	3.48	0.35 (0.39)	2.7
9	14	23 775.35	2	14	1	23 769.18	6.17	0.272	3.48	0.73 (0.78)	11.2
9	15	23 814.34	2	15	1	23 816.93	−2.59	0.272	3.48	1.31 (1.41)	32.1
9	16	23 855.92	2	16	1	23 868.25	−12.33	0.272	3.48	0.40 (0.49)	3.6
9	17	23 900.08	2	17	1	23 922.68	−22.61	0.272	3.48	0.22 (0.26)	1.2
10	53	28 309.05	2	53	2	28 281.76	27.29	0.231	2.96	0.13	0.6
10	54	28 443.79	2	54	2	28 457.78	−13.99	0.231	2.96	0.26	2.1
10	57	28 862.01	2	57	1	28 825.70	36.31	0.231	2.96	0.10	0.3
10	58	29 006.05	2	58	1	29 017.72	−11.67	0.231	2.96	0.31	2.9
11	40	27 904.67	3	40	2	27 874.45	30.23	0.257	3.29	0.15	0.6
11	41	28 006.88	3	41	2	28 012.19	−5.31	0.257	3.29	0.75	12.9
11	42	28 111.49	3	42	2	28 149.21	−37.71	0.257	3.29	0.12	0.4
11	44	28 327.90	3	44	1	28 292.35	35.55	0.257	3.29	0.13	0.4
11	45	28 439.68	3	45	1	28 436.18	3.50	0.257	3.29	1.01	22.0
11	46	28 553.83	3	46	1	28 586.49	−32.66	0.257	3.29	0.14	0.5
12	21	27 555.44	4	21	2	27 533.32	22.12	0.242	3.10	0.18	1.0
12	22	27 610.22	4	22	2	27 604.91	5.30	0.242	3.10	0.67 (0.90)[h]	11.9
12	23	27 667.46	4	23	2	27 681.78	−14.32	0.242	3.10	0.28 (0.49)	2.2
12	26	27 853.92	4	26	1	27 841.40	12.51	0.242	3.10	0.31 (0.07)[i]	2.8
12	27	27 920.97	4	27	1	27 926.45	−5.48	0.242	3.10	0.66 (0.43)[i]	11.3
12	28	27 990.46	4	28	1	28 016.06	−25.60	0.242	3.10	0.16 (0.35)[i]	0.7

[a]Calculated with the constants from this work in Table V and after subtraction of 924.102 cm^{-1}, which is the zero point energy of $X^1\Sigma_g^+$ v = 0 from Ref. 3.

[b]Calculated with the constants from Ref. 13 and the addition of 613.650 cm^{-1}, which is the energy gap between v = 0 of $a^3\Pi_u$ and $X^1\Sigma_g^+$ from Ref. 3.

[c]Energy difference $\Delta = E_B - E_d$.

[d]Overlap integrals calculated with Le Roy's "LEVEL" program (Ref. 22).

[e]Off-diagonal spin-orbit interaction $W = |A_{dB}\langle v_B|v_d\rangle|$, where $|A_{dB}| = 8.3(1)$ cm^{-1} is an averaged value from Table XI.

[f]Perturbation shift $\delta = \sqrt{(\Delta/2)^2 + W^2} - |\Delta/2|$. Values in parentheses are from the observation.

[g]Contribution (squared coefficient) ratio $r = 1/(1 + \Delta/\delta)$ for $B^1\Delta_g$ to $d^3\Pi_g$, calculated for comparison with the intensity ratio of the forbidden transition to the allowed ones in Table XI.

[h]Reassigned by this work.

[i]Assigned by this work.

TABLE XI. Observed forbidden and allowed transitions at level crossing of the $B^1\Delta_g$ and $d^3\Pi_g$ states.

	$B^1\Delta_g$–$a^3\Pi_u$ (forbidden)		$d^3\Pi_g$–$a^3\Pi_u$ (allowed)						
J'-J''	v′-v″	υ (cm^{-1})	v′-v″	F'-F''	υ (cm^{-1})	δ[a]	W[b]	$\lvert A_{dB}\rvert$[c]	r(%)[d]
41-40	8-0(F_1)	21 421.436	1-0	1-1	21 426.120	0.92	1.94	8.78	(4.6)[e]
41-40	8-1(F_1)	19 829.205	1-1	1-1	19 833.893	0.74	1.70	7.70	15.8
9-8	9-1(F_2)	21 272.042	2-1	2-2	21 266.761	−1.08	2.09	7.68	27.4
9-10	9-1(F_2)	21 211.265	2-1	2-2	21 205.888	−1.13	2.15	7.90	(39)[e]
9-8	9-3(F_2)	18 108.320	2-3	2-2	18 103.004	−1.16	2.19	8.04	19.7
10-9	9-0(F_2)	22 884.228	2-0	2-2	22 890.465	0.92	2.22	8.16	(69)[e]
10-11	9-0(F_2)	22 816.427	2-0	2-2	22 822.567	0.94	2.25	8.26	(45)[e]
10-9	9-1(F_2)	21 267.868	2-1	2-2	21 273.930	0.92	2.22	8.16	13.6
10-11	9-1(F_2)	21 200.641	2-1	2-2	21 206.702	0.91	2.20	8.10	13.6
10-9	9-2(F_2)	19 674.611	2-2	2-2	19 680.722	0.92	2.22	8.16	(45)[e]
10-9	9-3(F_2)	18 104.737	2-3	2-2	18 110.848	0.92	2.22	8.16	12.1
10-11	9-3(F_2)	18 038.934	2-3	2-2	18 045.050	0.93	2.23	8.21	(4)[e]
14-13	9-1(F_1)	21 297.543	2-1	1-1	21 289.964	−0.78	2.33	8.56	(22)[e]
14-13	9-2(F_1)	19 705.519	2-2	1-1	19 697.852	−0.80	2.36	8.68	5.5
14-13	9-3(F_1)	18 136.748	2-3	1-1	18 129.098	−0.80	2.36	8.68	8.3
15-14	9-0(F_1)	22 907.132	2-0	1-1	22 912.822	1.37	2.33	8.56	(58)[e]
15-14	9-2(F_1)	19 700.759	2-2	1-1	19 706.228	1.40	2.36	8.69	25.1
15-14	9-3(F_1)	18 132.439	2-3	1-1	18 137.933	1.40	2.36	8.69	28.0
15-16	9-3(F_1)	18 040.876	2-3	1-1	18 046.302	1.33	2.28	8.39	(12)[e]

[a]Perturbation shift between observation and calculation for the allowed (Swan band) transition in cm^{-1}.
[b]$W = \sqrt{\delta(\delta + |\Delta|)}$, where Δ was taken from Table X.
[c]$|A_{dB}| = W/|\langle v_B|v_d\rangle|$, where $|\langle v_B|v_d\rangle|$ was taken from Table X.
[d]Observed intensity ratio of the forbidden transition to the allowed ones in percentage.
[e]Incorrect ratio due to the overlapped line intensity for the allowed or forbidden transitions.

large effect on the lower vibrational levels in $B'^1\Sigma_g^+$, are a direct result of the avoided crossing between the two states with the same $^1\Sigma_g^+$ symmetry. The assumption for the "original" $\omega_e x_e = 12$ cm^{-1} in both the $B'^1\Sigma_g^+$ and $X^1\Sigma_g^+$ states is just a crude approximation. The two "original" potential curves may just approach each other closely instead of crossing, but the two potential curves should also be distorted mutually by the near-avoided-crossing. The distortion should also affect the higher order anharmonic constants in both the $B'^1\Sigma_g^+$ and $X^1\Sigma_g^+$ states and a detailed simultaneous analysis of the two states is required to determine all the parameters quantitatively. High-level *ab initio* calculations take this interaction into account automatically and therefore obtain reasonable estimates for the observed $\omega_e x_e$ values.[7,8]

B. Perturbation near the level crossing of $B^1\Delta_g$ and $d^3\Pi_g$

For finding the perturbations between the $B^1\Delta_g$ and $d^3\Pi_g$ states, we plotted the rovibrational levels of the two states between 20 000 and 30 000 cm^{-1} in Fig. 4 and listed the term values of the levels around the level crossing in Table X. The $B^1\Delta_g$ state has $\Omega = 2$ and the $d^3\Pi_g$ state has $\Omega = 2$, 1, and 0 which correspond to the F_1, F_2, and F_3 spin components, respectively, so the F_3 component of $d^3\Pi_g$ does not interact with the $B^1\Delta_g$ state because $\Delta\Omega = 2$. The term values in Table X were calculated without considering the perturbation interactions, and the perturbation shift and the intensity ratio of the forbidden to the allowed transitions borrowed from the level mixing in Table X were estimated with the perturbation treatment for interaction between only two levels,[21] that is, two levels separated by Δ before interaction are shifted up and down by $\delta = \sqrt{(\Delta/2)^2 + W^2} - |\Delta/2|$ due to the interaction W, and the mixed wave functions have a contribution (squared coefficients) ratio of the parent state to the perturber as $1 + \Delta/\delta$. The v = 0 level of the $d^3\Pi_g$ state does not cross $B^1\Delta_g$ v = 6 and perturbs it only slightly as observed in this work. $d^3\Pi_g$ v = 0 F_2 crosses $B^1\Delta_g$ v = 7 around $J = 51$, which leads to a 0.43 cm^{-1} shift predicted in Table X, as compared with the 0.56 cm^{-1} perturbation observed.[13] A possible observation for the corresponding forbidden transitions at a lower wavenumber of $|\Delta| + 2\delta = 3.1$ cm^{-1} from the allowed ones is predicted with a 16% intensity of the allowed one, which was not identified due to some overlapping lines.

In this way, many perturbations observed previously[13] or rechecked by this work were confirmed as shown in Table X. For $d^3\Pi_g$ v = 2, the calculated perturbations around the crossing levels of $B^1\Delta_g$ v = 9 were all confirmed and the predicted forbidden transitions from $B^1\Delta_g$ v = 9 to $a^3\Pi_u$ were identified as shown in Table XI, among which several forbidden transitions corresponding to the allowed ones for $J = 9$ of $d^3\Pi_g$ v = 2 were noted previously without knowing the $B^1\Delta_g$ v = 9 perturber.[13] In Figs. 5 and 6, several identified pairs of allowed and forbidden transitions are shown. For the individual pairs of the forbidden and allowed transitions in Table XI, the interaction W was determined and the off-diagonal spin-orbit constant $|A_{dB}|$ was obtained by $W = |A_{dB}\langle v_B|v_d\rangle|$, where the overlap integrals were calculated with Le Roy's "LEVEL" program.[22] Finally, an average value $|A_{dB}| = 8.3(1)$ cm^{-1} is obtained. The perturbations around

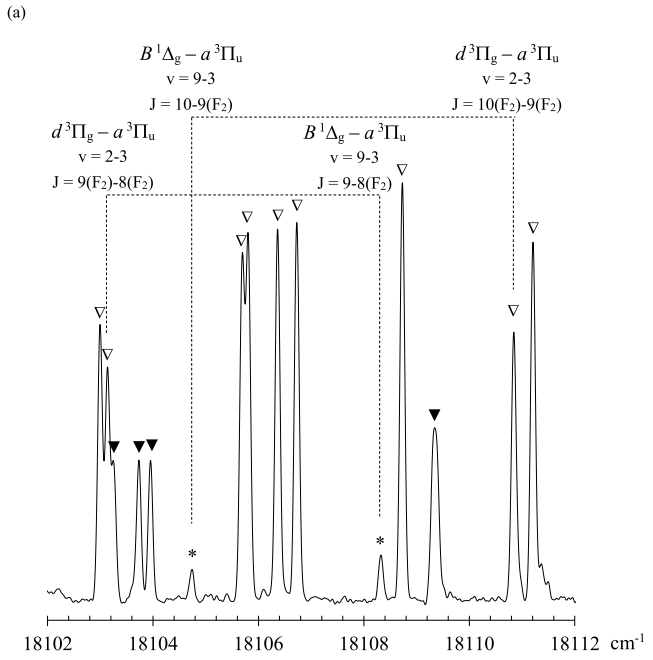

FIG. 5. Two short sections of spectra, (a) and (b), that show forbidden transitions marked with * and corresponding allowed transitions for the perturbations between J = 9 and 10 of $d^3\Pi_g$ v = 2 and $B^1\Delta_g$ v = 9. The $d^3\Pi_g$–$a^3\Pi_u$ transitions are marked with ∇ (assigned previously) and ▼ (assigned in this study as $P_3(33)$, $P_2(34)$, $P_1(35)$, and $P_1(36)$ overlapped with $P_2(35)$ of v = 2-3 from the left to the right in (a)).

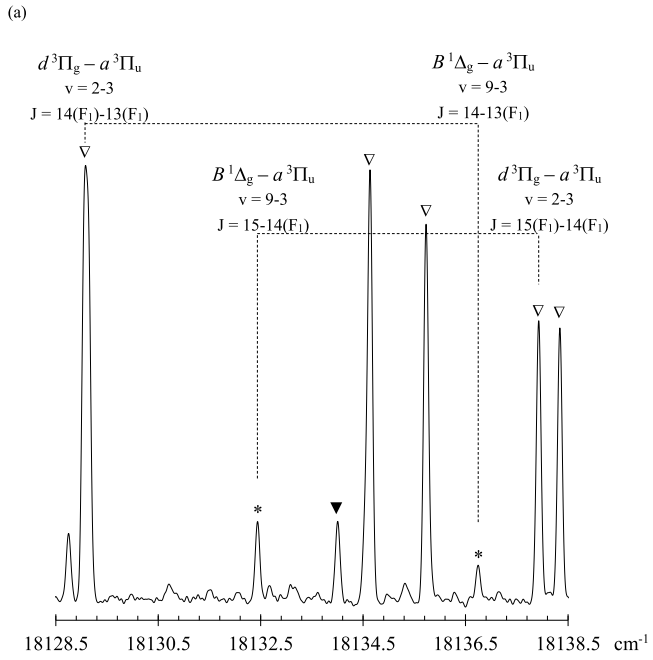

FIG. 6. More forbidden transitions and corresponding allowed transitions. The symbols have the same meaning as in Fig. 5. (▼ in (a) was assigned as P_3 (38) of v = 2-3 in this study.)

the level crossings of $d^3\Pi_g$ v = 2 and $B^1\Delta_g$ v = 10 and of $d^3\Pi_g$ v = 3 and $B^1\Delta_g$ v = 11 could not be confirmed since such high J transitions were not assigned. As for the perturbations around the level crossings of $d^3\Pi_g$ v = 4 and $B^1\Delta_g$ v = 12, several perturbed transitions were found but with quite different perturbation shifts from the calculation as shown in Table X. This could be because the prediction for $B^1\Delta_g$ v = 12 was not reliable since the observations were for transitions up to $B^1\Delta_g$ v = 8 and also because of the heavy perturbations in the $d^3\Pi_g$ v = 4 level, which means that the molecular constants were obtained from only a few high J transitions.[13]

V. CONCLUSIONS

Assignments for the $B'^1\Sigma_g^+$–$A^1\Pi_u$ and $B^1\Delta_g$–$A^1\Pi_u$ systems of C_2 have been extended to higher vibrational levels of the $B'^1\Sigma_g^+$ and $B^1\Delta_g$ states. The anharmonic constant $\omega_e x_e$ of nearly zero obtained for $B'^1\Sigma_g^+$ indicates a distortion of the potential curve and was explained as the result of an avoided

crossing or a nearly avoided crossing with the $X^1\Sigma_g^+$ state. If an avoided crossing occurs, a nonadiabatic transition between the adiabatic $B'^1\Sigma_g^+$ and $X^1\Sigma_g^+$ potential curves should be possible for a rapid passage through the crossing region as a Landau-Zener transition,[23] which may be used to check the existence of this avoided crossing. The difficulty is that the two potential curves do not result in different products but converge to the same dissociation limit.

The higher vibrational levels of the $B^1\Delta_g$ state were found to be responsible for the many perturbations in the $d^3\Pi_g$ state observed previously for the Swan band system. As proof, many forbidden transitions were identified at the level crossings. There are more level crossings between the $d^3\Pi_g$ and $B^1\Delta_g$ states for higher vibrational and rotational levels, which will lead to more perturbations and more forbidden transitions to be observed.

ACKNOWLEDGMENTS

This work was supported by JSPS KAKENHI under Grant No. 15K05391. Some support was also provided by the NASA laboratory astrophysics program.

[1]P. Bornhauser, Y. Sych, G. Knopp, T. Gerber, and P. P. Radi, J. Chem. Phys. **134**, 044302 (2011).
[2]M. Nakajima and Y. Endo, J. Mol. Spectrosc. **302**, 9 (2014); **305**, 48 (2014).
[3]W. Chen, K. Kawaguchi, P. F. Bernath, and J. Tang, J. Chem. Phys. **142**, 064317 (2015).
[4]P. Bornhauser, R. Marquardt, C. Gourlaouen, G. Knopp, M. Beck, T. Gerber, J. A. van Bokhoven, and P. P. Radi, J. Chem. Phys. **142**, 094313 (2015).
[5]J. G. Phillips, J. Mol. Spectrosc. **28**, 233 (1968).
[6]M. Douay, R. Nietmann, and P. F. Bernath, J. Mol. Spectrosc. **131**, 261 (1988).
[7]D. Shi, X. Zhang, J. Sun, and Z. Zhu, Mol. Phys. **109**, 1453 (2011).
[8]J. S. Boschen, D. Theis, K. Ruedenberg, and T. L. Windus, Theor. Chem. Acc. **133**, 1425 (2014).
[9]P. M. Goodwin and T. A. Cool, J. Mol. Spectrosc. **133**, 230 (1989).
[10]Y. Bao, R. S. Urdahl, and W. M. Jackson, J. Chem. Phys. **94**, 808 (1991).
[11]O. Sorkhabi, V. M. Blunt, H. Lin, D. Xu, J. Wrobel, R. Price, and W. M. Jackson, J. Chem. Phys. **107**, 9842 (1997).
[12]T. Wakabayashi, A.-L. Ong, and W. Krätschmer, J. Chem. Phys. **116**, 5996 (2002).
[13]A. Tanabashi, T. Hirao, T. Amano, and P. F. Bernath, Astrophys. J., Suppl. Ser. **169**, 472 (2007).
[14]P. N. Ghosh, M. N. Deo, and K. Kawaguchi, Astrophys. J. **525**, 539 (1999).
[15]M. Douay, R. Nietmann, and P. F. Bernath, J. Mol. Spectrosc. **131**, 250 (1988).
[16]See supplementary material at http://dx.doi.org/10.1063/1.4940907 for total line list of the global analysis on the $B^1\Delta_g$–$A^1\Pi_u$ system.
[17]G. Herzberg, *Molecular Spectra and Molecular Structure, Spectra of Diatomic Molecules*, 2nd ed. (Van Nostrand-Reinhold, New York, 1950), Vol. 1, p. 108.
[18]M. Nakajima and Y. Endo, J. Chem. Phys. **139**, 244310 (2013).
[19]R. J. Le Roy, "RKR1 2.0: A Computer Program Implementing the First-Order RKR Method for Determining Diatomic Molecule Potential Energy Functions," University of Waterloo Chemical Physics Research Report CP-657R, See the "Computer Programs" link at http://leroy.uwaterloo.ca/programs 2004.
[20]G. Herzberg, *Molecular Spectra and Molecular Structure, Spectra of Diatomic Molecules*, 2nd ed. (Van Nostrand-Reinhold, New York, 1950), Vol. 1, p. 295.
[21]L. D. Landau and E. M. Lifshitz, *Quantum Mechanics: Non-Relativistic Theory*, 3rd ed. (Butterworth-Heinemann, Oxford, 1977), p. 140.
[22]R. J. Le Roy, "LEVEL 7.7: A Computer Program for Solving the Radial Schrödinger Equation for Bound and Quasibound Levels," University of Waterloo Chemical Physics Research Report CP-661, See the "Computer Programs" link at http://leroy.uwaterloo.ca/programs 2005.
[23]J. R. Rubbmark, M. M. Kash, M. G. Littman, and D. Kleppner, Phys. Rev. A **23**, 3107 (1981).